Two-dimensional dispersion-managed light bullets in Kerr media

M. Matuszewski,[1] M. Trippenbach,[1] B. A. Malomed,[2] E. Infeld,[3] and A. A. Skorupski[3]
[1]*Physics Department, Warsaw University, Hoża 69, PL-00-681 Warsaw, Poland and Soltan Institute for Nuclear Studies, Hoża 69, PL-00-681 Warsaw, Poland*
[2]*Department of Interdisciplinary Sciences, Faculty of Engineering, Tel Aviv University, Tel Aviv 69978, Israel*
[3]*Physics Department, Warsaw University, Hoża 69, PL-00-681 Warsaw, Poland*
(Received 5 February 2004; published 7 July 2004)

We propose a scheme for stabilizing spatiotemporal solitons (STSs) in media with cubic self-focusing nonlinearity and "dispersion management," i.e., a layered structure inducing periodically alternating normal and anomalous group-velocity dispersion. We develop a variational approximation for the STS, and verify results by direct simulations. A stability region for the two-dimensional (2D) STS (corresponding to a planar waveguide) is identified. At the borders between this region and that of decay of the solitons, a more sophisticated stable object, in the form of a periodically oscillating bound state of two subpulses, is also found. In the 3D case (bulk medium), all the spatiotemporal pulses spread out or collapse.

DOI: 10.1103/PhysRevE.70.016603 PACS number(s): 42.65.Tg, 42.50.Md

I. INTRODUCTION

Spatiotemporal solitons (STSs) in optics, dubbed "light bullets" [1], have attracted a great deal of attention, as they are promising objects for both fundamental [2–6] and applied [7,8] research. While stationary solutions for STSs in the corresponding mathematical models, such as the multidimensional cubic nonlinear Schrödinger (NLS) equation, can be easily found [1], the real challenge is posed by their stability. In particular, all the solitons in the spatially uniform NLS (or $\chi^{(3)}$) model are unstable because of the occurrence collapse [9]. A way around this problem is the use of a weaker nonlinearity, such as saturable [7], cubic-quintic [10], quadratic ($\chi^{(2)}$) [2–6], or that induced by the self-induced transparency [11].

To date, neither three-dimensional (3D) STSs in a bulk medium nor their 2D counterparts in a planar waveguide have been observed in experiment. The only experimental finding reported thus far was in the form of stable quasi-2D solitons in 3D crystals with the $\chi^{(2)}$ nonlinearity (i.e., solitons which fail to confine themselves in one transversal direction). In fact, even this soliton, if created farther from the threshold, may be subject to a different instability, viz., modulational instability developing along its uniform direction [12]. On the other hand, it was predicted [6] that a 2D spatial cylindrical soliton can be quite effectively stabilized in a bulk *layered* medium, with opposite signs of the Kerr coefficient in adjacent layers, corresponding to self-focusing and self-defocusing, respectively. A similar effect was then predicted for what may be regarded as 2D STSs in Bose-Einstein condensates (BECs), with the sign in front of the cubic nonlinear term subject to periodic sinusoidal modulation in time via the Feshbach resonance [13]. However, no stable 3D soliton could be found in either setting (optical or BEC) of this type. As to the $\chi^{(2)}$ media, it is relevant to mention that stable STSs can be readily predicted in a medium of "tandem" type, composed of alternating linear and quadratically nonlinear layers [14].

Serious difficulties encountered in the experimental search for STS in $\chi^{(2)}$ optical crystals suggest looking for alternative settings where "light bullets" may be expected. A possibility to support stable STS in the case of the ordinary Kerr ($\chi^{(3)}$) nonlinearity is to use a layered structure that does not affect the nonlinearity (in fact, it is very difficult to invert the sign of the Kerr coefficient), but rather gives rise to periodic reversal of the sign of local group-velocity dispersion (GVD). This is a common setting in fiber optics, known as "dispersion management" (DM), see, e.g., Refs. [15,16]; in particular, the world's first commercial fiber optic telecommunication link operating on solitons uses the DM technique [17]. As a straightforward multidimensional generalization, one can consider a layered medium (bulk or planar waveguide) of the same type, uniform in the transverse direction(s). The main result of this work is that STS are *stable* in this setting in the 2D (planar) case, but they cannot be stabilized in the 3D (bulk) case. In the 2D case, in addition to the ordinary stable single-peaked solitons, we will also demonstrate the existence of stable double-peaked oscillatory states, which are bound states of two subpulses generated by the splitting of an initial pulse.

The model outlined above is based on the normalized equation describing the evolution of the local amplitude u of the electromagnetic wave propagating along z (in suitably defined dimensionless units)

$$iu_z + (1/2)[\nabla_\perp^2 u + D(z)u_{\tau\tau}] + |u|^2 u = 0, \tag{1}$$

where the diffraction operator $\nabla_\perp^2$ acts on the transverse coordinate(s) x and y (in the 3D case), τ is the ordinary reduced temporal variable, and $D(z)$ is the same local GVD coefficient as in the usual DM models [15,16]

$$D(z) = \begin{cases} D_+ > 0, & 0 < z < L_+, \\ D_- < 0, & L_+ < z < L_+ + L_- \equiv L, \end{cases} \tag{2}$$

which repeats periodically with the period L. Note that Eq. (1) has a manifest property of Galilean invariance: if $u_0(x,z,\tau)$ is a solution, a two-parametric family of "boosted" (moving) solutions can be generated from it in the following form:

$$u(x,z,\tau)=\exp\left[i\left(qx-\omega\tau-\frac{1}{2}q^2z-\frac{1}{2}\omega^2\int D(z)dz\right)\right]\times u_0\left(x-qz,z,\tau+\omega\int D(z)dz\right), \tag{3}$$

where q and ω are two arbitrary real parameters ("Galilean boosts").

To cast the model into a normalized form, we set, by means of obvious rescalings, $D_+\equiv 1, L\equiv 2$. The ratio L_+/L_- remains an irreducible parameter, but it is well known that, in the usual DM model (for optical fibers), the results do not depend on this ratio, nor separately on the soliton's temporal width $T_{\rm FWHM}$, but rather on the combination known as the DM strength [15], $S\equiv(D_+L_++D_-L_-)/T_{\rm FWHM}^2$. Therefore, in this paper we report results obtained for $L_+=L_-=1$ (we have checked that the results are indeed very close for other values of L_+/L_-). Then, the only remaining free parameter of the DM map (2) is the path-average dispersion (PAD)

$$\overline{D}\equiv(D_+L_++D_-L_-)/L=(1+D_-)/2, \tag{4}$$

with regard to $D_+=1, L_\pm=1$. The remaining parameter D_- can be expressed in terms of $\overline{D}$: as it follows from Eq. (4), $D_-=2\overline{D}-1$.

It is relevant to mention that a 2D model somewhat similar to the one defined above was recently introduced in Ref. [18]; it differs by sinusoidal modulation of $D(z)$, instead of the piecewise constant mode adopted in Eq. (2) and, most importantly, by the fact that (in the present notation) it has the same modulated coefficient $D(z)$ multiplying both the GVD term $u_{\tau\tau}$ and the diffraction one u_{xx}. In fact, the model introduced in Ref. [18] was motivated by a continuum limit of some discrete models; in the present context, it would be quite difficult to introduce the periodic reversal of the sign of the transverse diffraction. From the standpoint of the model proper, there is a great difference between Eq. (2), which is strongly anisotropic in the plane (x,τ), and the isotropic equation introduced in Ref. [18].

The rest of the paper is organized as follows. In Sec. II we report results for the 2D case. By means of both the variational approximation (VA) and direct simulations, we demonstrate the existence of stable 2D STSs; stable double-peaked oscillatory states are also reported in this section. The 3D case is considered in Sec. III, with the opposite conclusion—no stable solitons can be found in that case (for which we propose a simple explanation). Section III concludes the paper.

II. THE TWO-DIMENSIONAL CASE

A. Variational approximation

In the case of the planar-waveguide model, $\nabla_\perp^2$ in Eq. (1) is replaced by $\partial^2/\partial x^2$. First, we aim to apply the variational approximation to a search for STS solutions (a review of this method can be found in Ref. [16]). To this end, we adopt a straightforward Gaussian ansatz

$$u=A(z)\exp\left\{i\phi(z)-\frac{1}{2}\left[\frac{x^2}{W^2(z)}+\frac{\tau^2}{T^2(z)}\right]+\frac{i}{2}[b(z)x^2+\beta(z)\tau^2]\right\}, \tag{5}$$

where A and ϕ are the amplitude and phase of the soliton, W and T are its transverse and temporal widths (the latter is related to the abovementioned full width at half maximum as follows: $T_{\rm FWHM}=2\sqrt{\ln 2}T$), and b and β are the spatial and temporal chirps. The Lagrangian from which the 2D version of Eq. (2) is derived is $L=(1/2)\int_{-\infty}^{+\infty}[i(u_zu^*-u_z^*u)-|u_x|^2-D|u_\tau|^2+|u|^4]dxd\tau$. Substitution of the ansatz (5) into the Lagrangian yields an effective Lagrangian

$$(4/\pi)L_{\rm eff}=A^2WT[4\phi'-b'W^2-\beta'T^2-W^{-2}-DT^{-2}+A^2-b^2W^2-D(z)\beta^2T^2], \tag{6}$$

where the prime stands for d/dz.

The variational equation $\delta L/\delta\phi=0$, applied to the expression (6), yields the energy-conservation relation $dE/dz=0$, where

$$E\equiv A^2WT. \tag{7}$$

Equation (7) is used to eliminate A^2 in favor of the constant E. Then, the term $\sim\phi'$ in the Lagrangian may be dropped, and it takes the form

$$\frac{4L_{\rm eff}}{\pi E}=-b'W^2-\beta'T^2-\frac{1}{W^2}-\frac{D(z)}{T^2}+\frac{E}{WT}-b^2W^2-D(z)\beta^2T^2. \tag{8}$$

Varying the latter expression with respect to W,T and b,β yields the following system of equations:

$$b=W'/W,\quad \beta=D^{-1}T'/T, \tag{9}$$

$$W''=\frac{1}{W^3}-\frac{E}{2W^2T}, \tag{10}$$

$$T''-\frac{D'}{D}T'=\frac{D^2}{T^3}-\frac{DE}{2WT^2}. \tag{11}$$

We note in passing that, as is well known [19], in the case of $D=\text{const}>0$, fixed-point (FP) solutions to the VA equations (9)–(11) are degenerate: the FP exists at a single value of the energy $E=2\sqrt{D}$ and, at this special value of E, there is a family of FPs with $T=\sqrt{D}W$ (W is arbitrary). These results exactly correspond to the existence of a special stationary soliton solution to the 2D isotropic NLS equation (the Townes soliton [9]), which exists at a single value of the energy, but with arbitrary width. All the abovementioned FPs are stable against small perturbations in the linear approximation, but feature a slowly (linearly, rather than exponentially) growing nonlinear instability.

In the case of the piecewise constant modulation corresponding to Eq. (2), the variables W, W', T, and β at junctions between the segments with $D=D_\pm$ must be continuous.

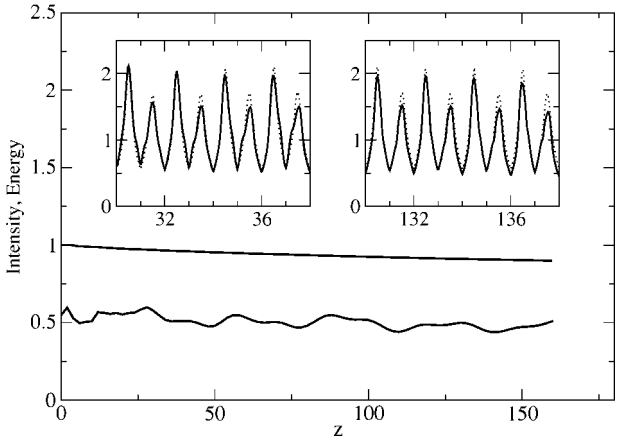

FIG. 1. The energy (upper curve) and peak power (squared amplitude) at the beginning of each cycle (lower curve) vs z, as found from direct simulations of the 2D equation (1), starting with the Gaussian pulse (13). Continuous lines in two insets display the evolution of the amplitude through a few cycles at early and later stages of the propagation. For comparison, the dotted lines show the same as found from the variational approximation. The system parameters are $D_+=-D_-=1$, $L_+=L_-=1$, and the parameters of the initial pulse are $T_0=1.35$, $W_0=1.35$, $E=1$, and $\beta_0=-1.85$.

As it follows from Eq. (9), the continuity of the temporal chirp $\beta(z)$ implies a jump of T' when passing from D_- to D_+, or vice versa:

$$(T')_{D=D_+} = (D_+/D_-)(T')_{D=D_-}. \tag{12}$$

B. Numerical results

We simulated both the variational equations (9)–(11), using the Runge-Kutta method, and the underlying NLS equation(1). In the latter case, the initial state was taken as per the ansatz (5), with zero spatial chirp (obviously, a point at which it vanishes can always be found, so this choice does not imply any special restriction):

$$u_0 = A_0 \exp\{-(1/2)[(x/W_0)^2 + (\tau/T_0)^2 - i\beta_0\tau^2]\}. \tag{13}$$

Numerical results are displayed in Figs. 1–7.

Figure 1 shows the evolution of the soliton's energy and peak power. Very slow decay of energy is due to transient emission of radiation from the pulse adjusting itself to the solitonic shape, the radiation being absorbed at boundaries of the simulation domain. The insets in Fig. 1 demonstrate how accurately the VA predicts results of the simulations. Further, Fig. 2 shows a sequence of the soliton's intensity distributions through one (40th) cycle of the evolution. The latter picture is very stable, remaining identically the same (for instance) at the 80th cycle, thus the 2D soliton is truly stable in the DM model. We stress that the actual shape of the pulse remains very close to a Gaussian, which helps to understand why the VA provides for good accuracy in this case. The evolution of the temporal width $T(z)$ for the same case, as predicted by the VA, is displayed in Fig. 3. On the contrary, the spatial width $W(z)$ remains nearly constant, suggesting that the stable 2D soliton may be construed, in loose terms,

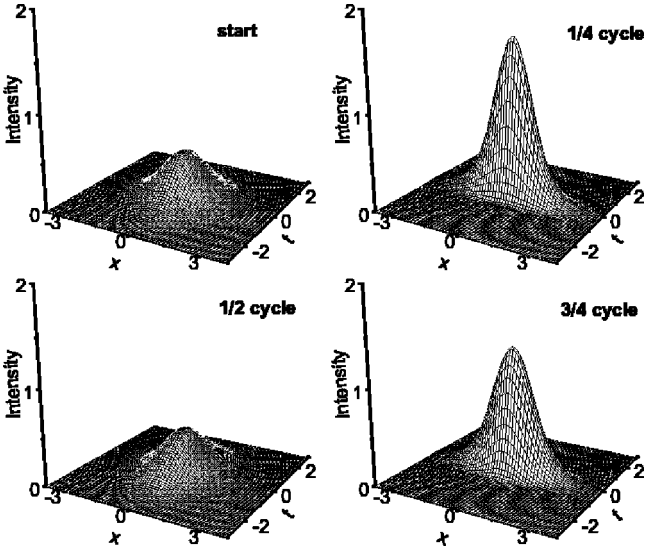

FIG. 2. Evolution the intensity distribution in the 2D soliton through the 40th cycle. Snapshots are taken at points corresponding to the start, 1/4, 1/2, and 3/4 of the cycle. Parameters are the same as in Fig. 1.

as a "product" of the temporal DM soliton in the τ direction, and ordinary spatial soliton localized in x (see Ref. [3]). We stress that no leakage from the established soliton is observed, up to the accuracy of the numerical simulations. This implies that a small amount of radiation, emitted from the pulse when it passes the normal-dispersion slice, is absorbed back into it in the slice with anomalous dispersion.

In some other cases, a periodic evolution occurs in a drastically different fashion: the initial pulse splits into two, which, however, do not fully separate, but rather form an oscillatory bound state, examples of which are shown in Figs. 4 and 5. In the case of Fig. 4, the VA still predicts a stable soliton in the form of a single Gaussian, while in the

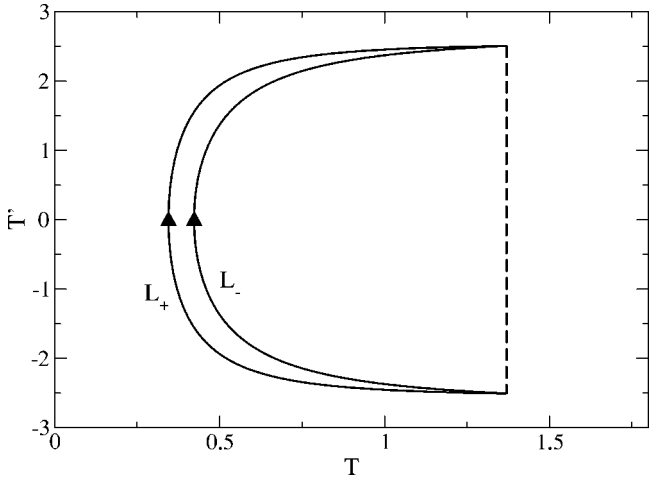

FIG. 3. A cycle of the soliton's evolution in the (T',T) plane according to the variational approximation, in the same case as shown in Figs. 1 and 2. The jump in T' occurs at the junction between L_+ and L_-, according to Eq. (12). Unlike the temporal width T, its spatial counterpart W remains almost constant within the cycle.

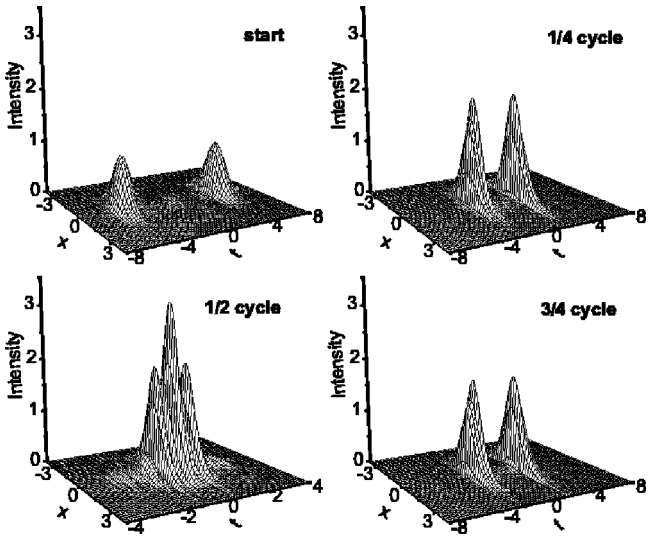

FIG. 4. The same as in Fig. 2, but for different parameters of the input pulse: $T_0=1$, $W_0=1$, $E=2$, and $\beta_0=0$. In this case, although the variational approximation predicts a stable single-peaked solution, the pulse splits up into an oscillatory bound state of two subpulses.

case of Fig. 5, VA predicts that the Gaussian-shaped soliton cannot self-trap (the initial width was the same in both cases). The actual behavior is similar in both cases: an initial Gaussian with zero chirp splits into two subpulses with chirps of opposite signs. After the establishment of stable oscillations, a recurring pattern is observed: while passing the layer with $D=D_+$, the subpulses approach each other and nearly merge; then, passing to the layer with $D=D_-$, they separate again and revert to the positions that they occupied at the beginning of the cycle.

The VA makes wrong predictions in these cases, as the simple Gaussian ansatz (5) is obviously irrelevant to describe

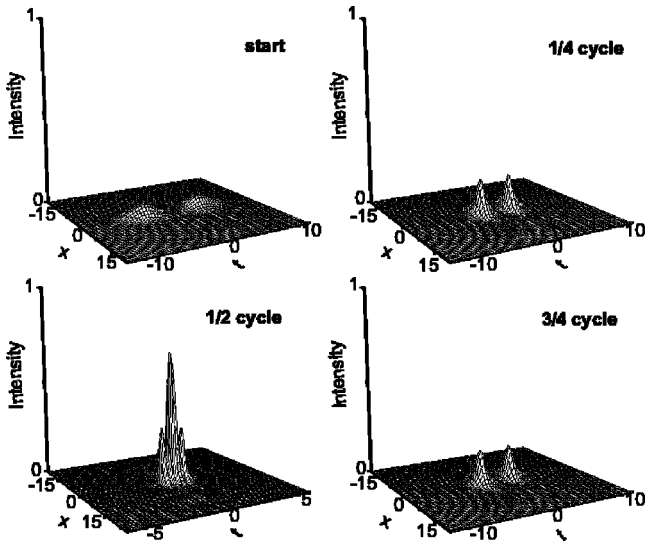

FIG. 5. The same as in Fig. 2, but for $\beta_0=0$. In this case, the variational approximation predicts single pulse decay, but, in fact, it evolves into two stable oscillatory bound states, as in the case of Fig. 4.

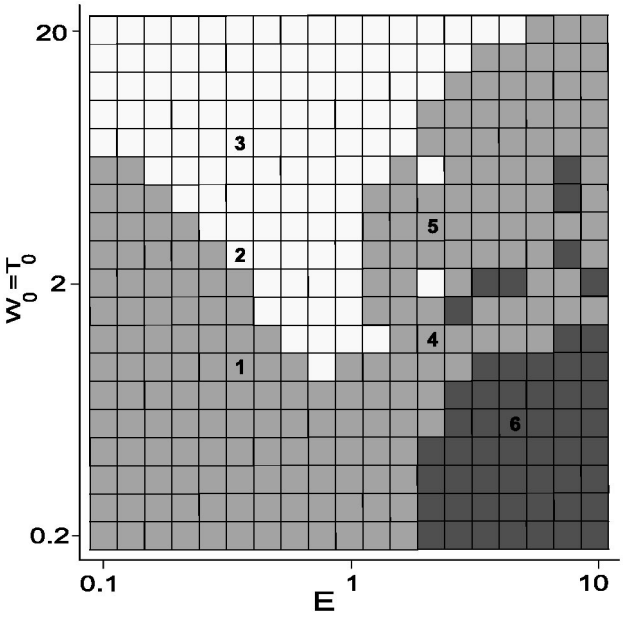

FIG. 6. The stability diagram in the plane (E,W_0) of the energy and width of the initial pulse, with $W_0=T_0$ and $\beta_0=0$. Predictions of the variational approximation are marked as follows: the stability region is unshaded, while ones where the pulse is unstable due to spreading out or collapse are shaded, respectively, gray and dark gray. The numbered points are those at which direct simulations of Eq. (1) were performed, to verify the predictions, as explained in the text.

the split pulses. It is relevant to mention that the splitting of an initial Gaussian is one of possible generic outcomes of the evolution in the ordinary (1D) DM model [16,20]. However, a cardinal difference is that no stable oscillatory bound states resulting from the splitting have been reported in the 1D

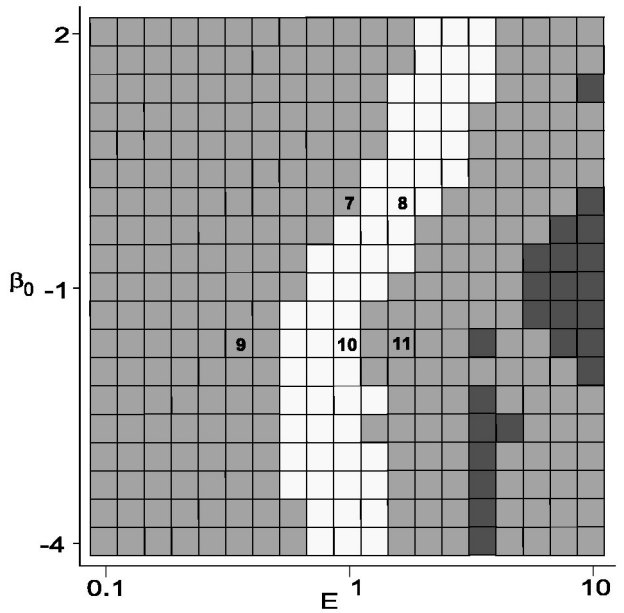

FIG. 7. The stability diagram in the plane (E,β_0) of the energy and temporal chirp of the initial pulse. Shading has the same meaning as in Fig. 6. The numbered points are explained in the text.

model. In this connection, it may be relevant to mention that a drastic difference of the splitting of 1D (temporal) pulses and their spatiotemporal counterparts was observed in a recent experimental work [22], which was dealing with the propagation of ultrashort spatiotemporal pulses in water. In this work, it was found that, while the pulse suffers on-axis splitting, its spatially integrated temporal profile remains *unsplit*.

The results outlined above are summarized in the form of stability diagrams for the 2D solitons, which are displayed in Figs. 6 and 7. The diagrams are generated on the basis of simulations of the variational equations (9)–(11), which are verified by direct simulations of Eq. (1) at sampling points indicated in the diagrams by digits. At points 1, 2, 3, 6, 9, and 10 the behavior predicted by the VA is confirmed by the simulations. At points 7 and 8, a periodic split-pulse evolution is observed. It is similar to that shown above in Figs. 4 and 5. Note that this behavior, which may be interpreted as an intermediate case between the stability and decay of a single-peaked soliton, is indeed observed close to VA-predicted borders between stable and decaying solitons.

At point 4, which is close to the VA-predicted border between decay and collapse, direct simulations initially demonstrate strong emission of radiation and broadening of the pulse, which eventually cease, being changed by seemingly chaotic oscillations of the localized pulse. There is no tangible energy loss. At point 5, essentially the same chaotic regime sets in, which is preceded, however, by a self-compression of the initial pulse, rather than by broadening. Lastly, at point 11, a strong transient emission of radiation is observed, similar to point 4, but the pulse keeps its Gaussian shape all the time, and regular periodic oscillations of the soliton finally set in. It may happen that, at an extremely long time scale, unaccessible for current simulations, chaotically oscillating solitons (observed at points 4 and 5) gradually relax towards a periodically oscillating soliton, through very weak continuing radiation loss.

III. THE THREE-DIMENSIONAL CASE

In three dimensions, we adopt the same ansatz for the soliton as in Eq. (5), with x replaced by the radial variable r in the (x,y) plane. The respective effective Lagrangian is [see Eq. (8)]

$$\frac{2L_{\rm eff}}{\pi^{3/2}E} = -b'W^2 - \frac{1}{2}\beta' T^2 - \frac{1}{W^2} - \frac{1}{2}\frac{D(z)}{T^2} + \frac{E}{2\sqrt{2}W^2T} - b^2W^2 - \frac{1}{2}D(z)\beta^2T^2, \tag{14}$$

and the variational equations are [see Eqs. (10) and (11)]

$$W'' = \frac{1}{W^3} - \frac{E}{2\sqrt{2}W^3T}, \tag{15}$$

$$T'' = \frac{[D(z)]^2}{T^3} - \frac{D(z)E}{2\sqrt{2}W^2T^2} \tag{16}$$

[the expressions for the chirps b and β have the same form as in Eq. (9)]. It is well known [19] that, in the 3D case with

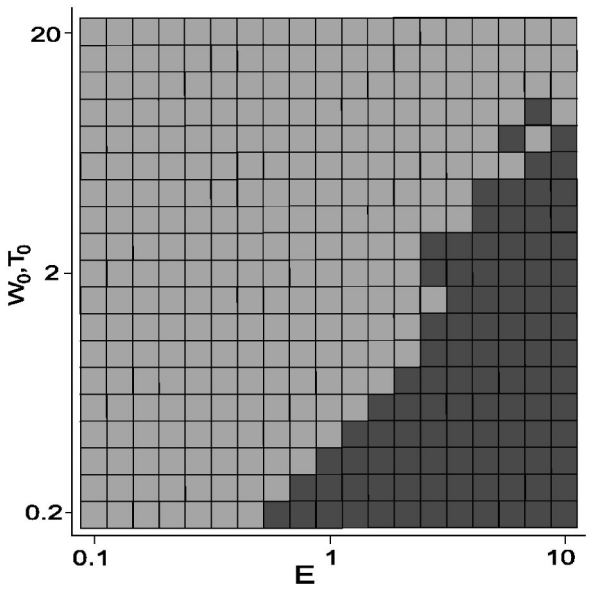

FIG. 8. The *instability* diagram for the solitons in the (E,W_0) parameter plane, as predicted by the variational approximation in the 3D case. Shading has the same meaning as in Fig. 6.

$D=\text{const}>0$, the FP of Eqs. (15) and (16), which is $W=E/(2\sqrt{2}D)$, $T=E/(2\sqrt{2})$, is subject to a linear (exponentially growing) instability, on the contrary to the weak nonlinear instability of the degenerate family of the FPs in the 2D case, see above. This difference corresponds to the fact that the 3D NLS equation gives rise to strong collapse, unlike the weak collapse in the 2D NLS equation [9].

Systematic simulations of Eqs. (15) and (16) have *never* produced a stable regime. Instead, they always give rise to collapse or decay of any initial pulse, as is shown in some detail in the "instability diagram," which is displayed in Fig. 8 (see Figs. 6 and 7 for the 2D case). In complete agreement with this prediction, direct simulations of the full 3D equation (1) could generate only either of these two outcomes, without revealing any stable solitonlike state. We also tried modulating both the dispersion as above and the nonlinearity, but the 3D soliton was still unstable. In fact, the absence of stable 3D solitons can easily be understood, as, in the transverse plane, the 3D equation (1) seems similar to the 2D NLS equation in a uniform medium, which may produce only the *unstable* Townes soliton [9].

IV. CONCLUSIONS

In this work, we have proposed a scheme for stabilizing spatiotemporal solitons in Kerr media with a layered structure. Unlike several recent works, which relied upon periodic alternation of the sign of the Kerr coefficient, we consider a more experimentally realistic possibility, viz., periodic reversal of the GVD sign, which resembles known dispersion-management (DM) schemes in fiber optics. First, we have developed the variational approximation (VA) based on the Gaussian ansatz for 2D and 3D STSs. In the 2D case, simulations of the resulting systems of coupled variational equations, which govern the evolution of the spatial and temporal

widths of the STS, reveal well-defined stability regions in the relevant parameter space. However, no stable states are predicted by the VA in the 3D case. Direct simulations of the full NLS equation produce quite similar results: no stable soliton in the 3D case, while in the 2D model the existence of the VA-predicted stability region is confirmed. Additionally, close to the borders between regions of stability and decay of the 2D STS, a more sophisticated stable state, in the form of a periodically oscillating bound state of two subpulses, is found.

The general conclusion that the DM scheme can stabilize 2D solitons, but not their 3D counterparts, is in qualitative agreement with results found in recent studies of other stabilized models, such as those for optical layered media with alternating sign of the Kerr coefficient [6], and for BECs controlled by means of the Feshbach resonance [13]. On the other hand, it seems quite feasible that *complete stabilization* of 3D STSs may be achieved if the DM in the longitudinal (temporal) direction is combined with a periodic spatial modulation of the refractive index in both, or maybe just one, transverse direction in the bulk medium. This possibility is suggested by recent results for stabilization of BEC solitons in 3D optical lattices [21], and will be considered in detail elsewhere.

ACKNOWLEDGMENTS

The authors acknowledge support from KBN through Grant No. 2P03 B4325 (M.M., M.T., E.I.). B.A.M. acknowledges the hospitality of the Physics Department and Soltan Institute for Nuclear Studies at Warsaw University, and partial support from the Israel Science Foundation through Grant No. 8006/03.

[1] Y. Silberberg, Opt. Lett. **15**, 1282 (1990).
[2] A. A. Kanashov and A. M. Rubenchik, Physica D **4**, 122 (1981).
[3] K. Hayata and M. Koshiba, Phys. Rev. Lett. **71**, 3275 (1993).
[4] B. A. Malomed, P. Drummond, H. He, A. Berntson, D. Anderson, and M. Lisak, Phys. Rev. E **56**, 4725 (1997); D. V. Skryabin and W. J. Firth, Opt. Commun. **148**, 79 (1998); D. Mihalache, D. Mazilu, B. A. Malomed, and L. Torner, *ibid.* **152**, 365 (1998); D. Mihalache, D. Mazilu, J. Dörring, and L. Torner, *ibid.* **159**, 129 (1999).
[5] X. Liu, L. J. Qian, and F. W. Wise, Phys. Rev. Lett. **82**, 4631 (1999); X. Liu, K. Beckwitt, and F. Wise, Phys. Rev. E **62**, 1328 (2000).
[6] I. Towers and B. A. Malomed, J. Opt. Soc. Am. B **19**, 537 (2002).
[7] D. E. Edmundson and R. H. Enns, Opt. Lett. **17**, 586 (1992); R. H. Enns, and S. S. Rangnekar, Phys. Rev. A **45**, 3354 (1992); R. H. Enns, D. E. Edmundson, S. S. Rangnekar, and A. E. Kaplan, Opt. Quantum Electron. **24**, S1295 (1992).
[8] R. McLeod, K. Wagner, and S. Blair, Phys. Rev. A **52**, 3254 (1995).
[9] L. Bergé, Phys. Rep. **303**, 260 (1998).
[10] A. Desyatnikov, A. Maimistov, and B. Malomed, Phys. Rev. E **61**, 3107 (2000); D. Mihalache *et al.*, Phys. Rev. Lett. **88**, 073902 (2002).
[11] M. Blaauboer, B. A. Malomed, and G. Kurizki, Phys. Rev. Lett. **84**, 1906 (2000); M. Blaauboer, G. Kurizki, and B. A. Malomed, Phys. Rev. E **62**, R57 (2000).
[12] X. Liu, K. Beckwitt, and F. Wise, Phys. Rev. Lett. **85**, 1871 (2000).
[13] H. Saito and M. Ueda, Phys. Rev. Lett. **90**, 040403 (2003); F. Kh. Abdullaev, J. G. Caputo, R. A. Kraenkel, and B. A. Malomed, Phys. Rev. A **67**, 013605 (2003).
[14] L. Torner, S. Carrasco, J. P. Torres, L.-C. Crasovan, and D. Mihalache, Opt. Commun. **199**, 277 (2001); L. Torner, IEEE Photonics Technol. Lett. **11**, 1268 (1999).
[15] A. Berntson, N. J. Doran, W. Forysiak, and J. H. B. Nijhof, Opt. Lett. **23**, 900 (1998).
[16] B. A. Malomed, Prog. Opt. **43**, 69 (2002).
[17] J. McEntee (unpublished).
[18] F. Kh. Abdullaev, B. B. Baizakov, and M. Salerno, cond-mat/0306244 (unpublished).
[19] M. Desaix, D. Anderson, and M. Lisak, J. Opt. Soc. Am. B **8**, 2082 (1991).
[20] R. Grimshaw, J. He, and B. A. Malomed, Phys. Scr. **53**, 385 (1996).
[21] B. B. Baizakov, B. A. Malomed, and M. Salerno, Europhys. Lett. **63**, 642 (2003).
[22] A. Matijosius, J. Trull, d P. Di Trapani, A. Dubietis, R. Piskarskas, A. Varanavicius, and A. Piskarskas, e-print physics/0312036.